

Temperature dependence of the Pd *K*-edge extended x-ray-absorption fine structure of PdC_x (*x* ~ 0.13)

James A. McCaulley

Hoechst Celanese Research Division, Robert L. Mitchell Technical Center, 86 Morris Avenue, Summit, New Jersey 07901

(Received 9 July 1992; revised manuscript received 8 September 1992)

Pd *K*-edge extended x-ray-absorption fine-structure (EXAFS) and x-ray-absorption near-edge-structure (XANES) measurements were performed on a Pd carbide phase, PdC_x (with *x* ~ 0.13), and metallic Pd powder at temperatures between 40 and 423 K. The data were analyzed by nonlinear least-squares fitting using an *ab initio* theoretical standard. The average lattice expansion of the carbide phase, 2.7±0.1% relative to Pd metal, agrees well with previous x-ray- and neutron-diffraction results. The temperature dependence of the Pd-Pd nearest-neighbor mean-squared relative displacement (σ^2) yields a Debye temperature, $\Theta_D = 295 \pm 10$ K for Pd powder. There is an additional static-disorder contribution in σ^2 of $0.0009 \pm 0.0002 \text{ \AA}^2$, relative to bulk Pd metal. The Debye temperature of PdC_{0.13} powder is also 295 ± 10 K. There is, however, an additional static-disorder contribution to σ^2 of 0.0012 \AA^2 , relative to Pd powder, probably the result of local distortion of the Pd lattice by interstitial C. The Pd-C coordination is not directly observed in a Fourier transform of the EXAFS. The location of C in octahedral interstices is evident by its effect, through multiple scattering, on the magnitude of the second Pd-Pd peak in the Fourier transform magnitude of the EXAFS data, which is greatly reduced. The Pd *K*-edge XANES spectrum of PdC_{0.13} is nearly identical to that of Pd metal. There is no significant chemical shift (≤ 0.5 eV) of the Pd *K* edge of PdC_{~0.13}.

I. INTRODUCTION

As early as 1970, expansion of the Pd lattice in supported Pd catalysts treated with C₂H₄ at high temperature was reported,¹ a finding that was later confirmed.² In both of these early reports it was erroneously concluded that Pd hydride had been formed. Nakamura and Yasui claimed that the "hydride" phase could be destroyed by treatment with oxygen at 150 °C.¹ Zaidi claimed that the "hydride" phase was responsible for selective synthesis of vinyl acetate.² These conclusions were later disproved when it was found that a Pd carbide phase (PdC_x, *x* ~ 0.13) was formed when Pd powder or foil was exposed to ethylene at high temperature.³ Although there is uncertainty in the literature concerning the maximum carbon content of this phase, reported values of *x*_{max} varying from 0.12 to 0.15, it will hereafter be assumed that *x* = 0.13 when referring to the sample used in this study. Destruction of the carbide phase by treatment with oxygen, under conditions similar to those reported by Nakamura and Yasui, was also demonstrated in that work. This has been followed by several studies of carbide formation in bulk Pd and supported Pd catalysts.⁴⁻⁸ Formation of a carbide phase in Pd catalysts is of interest because it suppresses Pd hydride formation which may in turn affect dissociative chemisorption of H-containing molecules. If dissociated hydrogen plays a role in reduction of supported Pd particles, formation of a carbide phase might increase the temperature required for reduction of Pd catalysts.

We have recently been investigating *in situ* formation of hydride and carbide phases in supported Pd catalysts using x-ray-absorption spectroscopy.⁹ Those studies prompted a detailed investigation of the x-ray-absorption

spectroscopy of Pd carbide to determine whether the carbide phase could be identified spectroscopically using evidence other than the lattice expansion. After completion of these experiments we learned of the work of Jones *et al.*^{10,11} who reported extended x-ray-absorption fine structure (EXAFS) results for PdC_x (*x* ~ 0.15) at 77 K. Here we report the temperature dependence of Pd *K*-edge absorption spectra of Pd and PdC_{0.13} powders over the temperature range 40–423 K.

II. EXPERIMENTAL PROCEDURES

PdC_x (*x* ~ 0.13) was prepared by heating a sample of Pd powder (Johnson Matthey No. 14622, 99.9% purity,

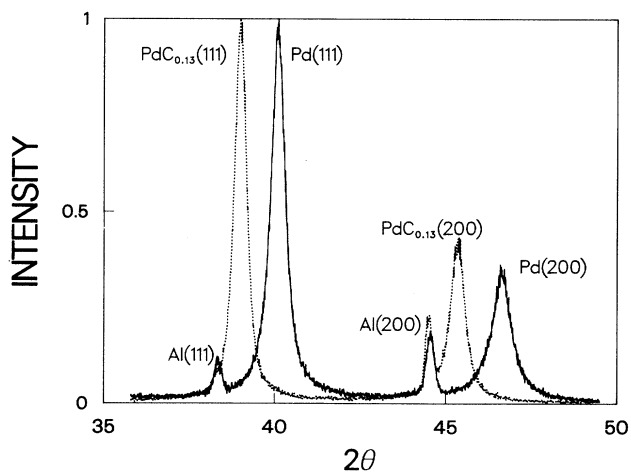


FIG. 1. XRD patterns from Pd (solid line) and PdC_{0.13} (dotted line) powders. Al peaks are from the sample holder. Ordinate units: arbitrary.

< 1 μm diameter) in a mixture of 1.0% C_2H_4 in Ar (MG Industries, certified mixture) at ambient pressure and 300 $^\circ\text{C}$ for 100 h. Complete conversion of Pd powder to PdC_x was verified by x-ray-diffraction (XRD). See Fig. 1. The Al peaks are from the sample holder. The lattice constants, 0.3890 and 0.3996 nm for Pd and PdC_x , agree well with published XRD and neutron scattering results.^{3,4} Carbide formation is diffusion limited⁶ and proceeds to completion in minutes at 150 $^\circ\text{C}$ in supported catalysts with an average Pd particle diameter of ~ 50 \AA .⁹

X-ray absorption samples of Pd and $\text{PdC}_{0.13}$ powders were prepared on Kapton tape (~ 20 layers). The K -edge step height, $\Delta\mu x$, where μx is the product of the absorption coefficient and sample thickness, was 0.7 and 0.5 for the Pd and $\text{PdC}_{0.13}$ samples, respectively. The total absorbance μx above the edge was ~ 0.9 and ~ 0.7 for the Pd and $\text{PdC}_{0.13}$ samples. The samples were mounted in a Cu sample holder and attached to the cold head of an Air Products Displex cryostat. In several experiments the temperature was measured with a Si diode at the end of the cold head. Later a second Si diode was mounted on the copper sample holder and the discrepancy between the two diodes was measured after allowing the sample temperature to equilibrate for at least 30 min. "Sample temperatures" that had been measured only at the cold head were corrected for this error. The estimated uncertainty of the sample temperature is ± 5 K. Measurements were made at 423 K by placing the tape samples in a homemade catalyst absorption cell (path length 12 mm) purged with argon.⁹

Pd K -edge ($E_K = 24\,350$ eV) absorption experiments were performed at the X-11A beam line of the National Synchrotron Light Source (NSLS) at Brookhaven National Laboratory.¹² The storage ring operated at 2.5 GeV with current between 100 and 230 mA. The monochromator was operated with two flat Si(111) crystals. It was not detuned to eliminate harmonics because the bending magnet source produces negligible flux at the third harmonic of the Pd K -edge energy and the Ar ionization chamber detectors are transparent at that energy. The calculated monochromator resolution ($\Delta E/E = 2 \times 10^{-4}$) at the Pd K edge is ~ 5 eV. Core hole lifetime broadening contributes ~ 7 eV, yielding a total resolution of ~ 8.5 eV. In several experiments the absorption spectrum of a pure Pd foil (25 μm thick) was measured (at ~ 300 K) simultaneously with the powder samples to accurately determine the position of the absorption edges in x-ray-absorption near-edge-structure (XANES) spectra of the powders. All x-ray-absorption measurements were performed in transmission mode, using flowing Ar ionization chambers to measure the incident intensity and the intensities transmitted through the powder samples and through the Pd reference foil.

III. DATA ANALYSIS

EXAFS data were analyzed using the University of Washington-Naval Research Laboratory (UW-NRL) EXAFS analysis programs; details are presented in Table I. The EXAFS function $\chi(k)$ was extracted by linear

TABLE I. Data analysis parameters.

Parameter	Value
E_0	24 350 eV
Data range	-200-1600 eV
Preedge linear fit range	-180-40 eV
Cubic spline range	50-1600 eV
Number of cubic spline segments	4
k weighting	3
Range of FT	2.5-19.0 \AA^{-1}
Hanning %	20%
Range of inverse FT	1.7-3.2 \AA
Hanning %	26%
Range of least-squares fit	3.0-19.0 \AA^{-1}
ΔE_0	-2.0-11.0 eV

preedge background subtraction, segmented cubic spline background subtraction above the edge, and step-height normalization. No energy-dependent normalization was applied to $\chi(k)$; an alternate approach is discussed below. The number of segments in the cubic spline fit was varied to reduce intensity in the Fourier transform (FT) magnitude plot below 1 \AA , while ensuring that the magnitude of the Pd-Pd nearest-neighbor peak was not decreased. E_0 (24 350 eV) was assumed to be at the first inflection point in K -edge spectrum; this is discussed further below. The unweighted EXAFS, $\chi(k)$, for Pd and $\text{PdC}_{0.13}$ at 40 K are presented in Fig. 2.

The k^3 -weighted EXAFS was Fourier transformed, yielding pseudoradial distribution functions such as those shown for Pd and $\text{PdC}_{0.13}$ in Fig. 3. The EXAFS from the first Pd-Pd coordination shell was isolated, and inverse Fourier transformed to obtain $k^3\chi_1(k)$.

The Fourier-filtered EXAFS from the Pd-Pd nearest neighbor was least-squares fitted in k space with a theoretical standard generated using the *ab initio* theoretical computer code FEFF (version 3.23).^{13,14} When fitting low-temperature Pd powder EXAFS data much better fits were obtained using FEFF standards than using 300-K

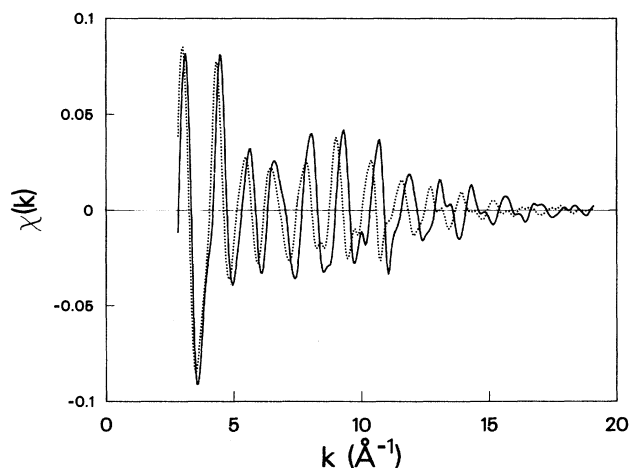


FIG. 2. Unweighted EXAFS from Pd (solid line) and $\text{PdC}_{0.13}$ (dotted line) powders at 40 K.

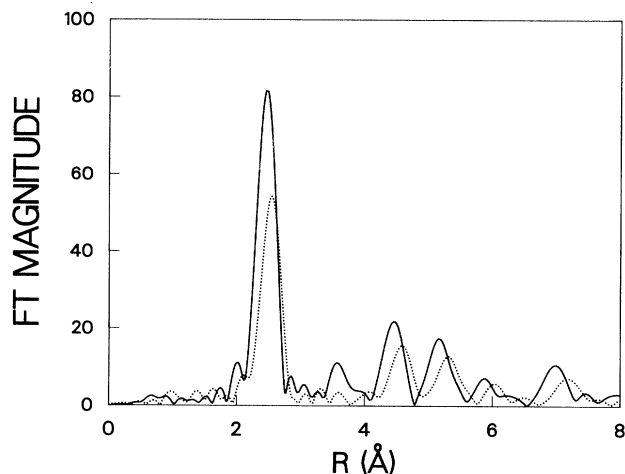


FIG. 3. Fourier transform magnitudes of k^3 -weighted EXAFS from Pd (solid line) and PdC_{0.13} (dotted line) powders at 40 K. Ordinate units: \AA^{-3} .

Pd foil data. A theoretical EXAFS spectrum, $\chi_1(k)$, was generated for the first Pd-Pd coordination shell in Pd metal at 300 K. The Pd-Pd distance used was 2.7505 \AA . The mean-squared relative displacement, $\sigma^2 = 0.0063 \text{\AA}^2$, was taken from the results of Yokoyama, Kimoto, and Ohta.¹⁵ The amplitude factor,¹³ S_0^2 , was taken to be 1.0; this yielded better results for Pd foil at 300 K than lower values. The theoretical $\chi(k)$ generated using FEFF was treated in the same manner as the experimental data through isolation of $k^3\chi_1(k)$. All the experimental Pd and PdC_{0.13} data were fitted using the theoretical standard with a fixed Pd-Pd coordination number, $N = 12$, and with $\Delta E_0 = -1.0$ or -2.0 eV (different values were used for data collected on two separate visits to NSLS). The assumed coordination number is justified by our observation that surface Pd oxide, which is easily observed in supported Pd catalysts (with an average coordination number less than 12) that have been exposed to air, is not detected. This indicates that the Pd particles are much larger in the powder than in typical supported catalysts and the EXAFS spectrum should be dominated by fully coordinated Pd atoms.

When comparing experimental and theoretical EXAFS data one usually performs an energy-dependent normalization of the background-subtracted experimental $\chi(E)$ spectrum. The energy-dependent normalization factor is $\mu(E)/\mu_0$ where $\mu(E)$ is the absorption coefficient, often taken from McMaster's tabulation,¹⁶ and μ_0 is the absorption coefficient just above the edge. As mentioned above, no energy-dependent normalization (i.e., McMaster correction) was applied to the $\chi(E)$ data. Instead, we used a procedure similar to that used by Rehr *et al.* when they compared *ab initio* theoretical EXAFS spectra to experimental spectra.¹³ They found that an energy-dependent normalization could be approximated well by an artificial "Debye-Waller" factor, $\exp(2\sigma_{MM}^2 k^2)$. This approach, which approximates $\mu(E)$ as an exponential function, is convenient because it reduces the energy dependence of μ above each absorption edge to a single

constant. For the Pd K edge we found $\sigma_{MM}^2 = 0.00021 \text{\AA}^2$. This factor was subtracted from σ^2 values obtained by least-squares fitting to Fourier-filtered EXAFS of Pd and PdC_{0.13} powders.

Analysis of the EXAFS data acquired for Pd foil at room temperature using the FEFF standard yielded a Pd-Pd distance of 2.732 \AA and a total Debye-Waller (DW) factor $\sigma^2 = 0.0060 \text{\AA}^2$, in fair agreement with the results of Yokoyama, Kimoto, and Ohta (2.747 \AA and 0.0063 \AA^2).¹⁵ Better agreement might have been obtained for the Pd-Pd distance if we had used a third-order cumulant expansion of the EXAFS equation.¹⁵ This is discussed further below.

Several variations of this analysis procedure were performed: different numbers of cubic spline segments, different k weighting, narrower FT, and inverse FT ranges. These variations did not significantly affect the results. In addition, least-squares fits were also performed allowing N to vary. Values of N obtained thereby ranged from 12.3 to 13.3 for Pd metal and 11.6 to 12.7 for PdC_{0.13}, with concomitant variations in σ^2 . The temperature dependence of σ^2 did not depend significantly on whether or not N was allowed to vary in the least-squares fits. The ratio fit method¹⁷ was also used to analyze the $k^3\chi_1(k)$ data for Pd powder, yielding results identical to those obtained by least-squares fitting.

XANES spectra were subjected to linear preedge background subtraction and normalization with respect to the intensity of the absorption maximum at ~ 40 eV, which was proportional to the step-height normalization factor used in the EXAFS analysis. The data were fitted with a smoothing spline from which the first and second derivatives were obtained.

IV. RESULTS AND DISCUSSION

A. EXAFS results

The FT magnitude plots in Fig. 3 are essentially identical to those presented by Jones *et al.*^{10,11} and reveal three facts about the x-ray-absorption spectroscopy of PdC_{0.13}: the Pd-C coordination is not directly observable in the FT magnitude, the first Pd-Pd coordination shell amplitude is $\sim 40\%$ smaller in PdC_{0.13}, and the second Pd-Pd coordination shell peak is much less intense, relative to the first Pd-Pd shell, than in Pd metal. The latter observation provides information on the location of C atoms in PdC_{0.13}. Although their FT plot also shows that the second Pd-Pd shell peak is much smaller in the PdC_{0.15} data, Jones *et al.* did not discuss it.

Using FEFF version 3.25, theoretical Pd-C EXAFS spectra were generated assuming various values of σ^2 (0.0–0.020 \AA^2) to simulate the expected Pd-C EXAFS in PdC. Fourier transformation of the k^3 -weighted EXAFS showed that a Debye-Waller factor significantly less than 0.001 \AA^2 (at 40 K) would be required for the Pd-C "shell" to be observed directly in the FT of the k^3 -weighted EXAFS from PdC_{0.13} powder. Attempts to emphasize the Pd-C coordination by limiting the FT to low k values and using k^1 weighting did not significantly improve its visibility.

Jones *et al.* reported that they isolated the Pd-C EXAFS by subtracting calculated Pd-Pd EXAFS (scaled to correct for lattice expansion) from the $\chi(k)$ obtained for PdC_{0.15}. Analysis of the resulting $\chi(k)$ difference file yielded Pd-C distances of 1.96 and 3.46 Å. A similar approach was used by Capehart, Mishra, and Pinkerton¹⁸ to isolate Sm-N EXAFS in Sm₂Fe₁₇N_x. To apply this method we first multiplied the $\chi(k)$ obtained for PdC_{0.17} at 40 K by $\exp(2k^2\sigma^2)$ with $\sigma^2=0.0012 \text{ \AA}^2$ (a structural disorder contribution to σ^2 of PdC_{0.13}, discussed below) to normalize the $\chi(k)$ amplitude. Unless such an amplitude normalization is performed, the difference file is dominated by Pd-Pd EXAFS; note the different amplitudes of $\chi(k)$ in Fig. 1. The k values of the PdC_{0.13} $\chi(k)$ data were then adjusted to correct for the measured lattice expansion of 2.7%. An interpolating cubic spline was used to extract values of the normalized $\chi(k)$ data for PdC_{0.13} on the same grid of abscissa values as the Pd powder $\chi(k)$ data. A difference file was obtained by subtracting Pd powder $\chi(k)$ data from the interpolated values of the normalized $\chi(k)$ function for PdC_{0.13}. The difference file was then Fourier transformed as described above. The FT magnitude of the difference file contained no discernible Pd-C peaks; it was dominated by imperfect subtraction of the Pd-Pd EXAFS. Likewise, taking the difference between Fourier-filtered EXAFS from PdC_{0.13} and a fit to that EXAFS using metal foil data yields a difference file with significant Pd-Pd EXAFS remaining. We cannot reproduce the difference file presented by Jones *et al.*,¹¹ which contains no noise above 4 Å.

The location of C in octahedral holes of the Pd lattice is confirmed by its effect on the EXAFS from the second Pd-Pd coordination shell. Lengeler has reported¹⁹ an increase of the second shell intensity in NiH_{0.85}, where H atoms occupy octahedral interstices in the fcc Ni lattice. Using Pd phase-corrected Fourier transforms, Lytle has

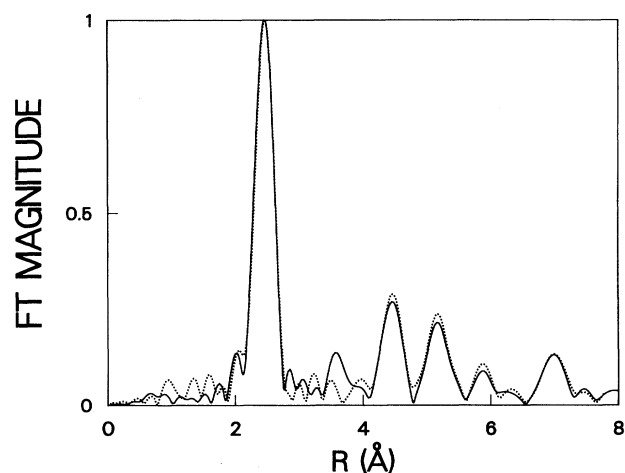


FIG. 4. Comparison of the FT magnitudes obtained for Pd and PdC_{0.13} at 40 K. Ordinate values have been normalized with respect to the intensity of the first Pd-Pd coordination shell; abscissa values of the PdC_{0.13} data have been divided by 1.027 to account for lattice expansion. Ordinate units: arbitrary.

observed a multiple scattering induced phase shift in the imaginary portion of the FT near the second Pd-Pd shell in Pd hydride.²⁰ Lengeler has also reported an increase in the intensity of the second Pd-Pd peak in the FT magnitude plot obtained for PdB_x ($x=0.115$ and 0.16).²¹ Figure 4 presents the FT magnitude plots for Pd and PdC_{0.13}, where the ordinate and abscissa have been scaled as described by Lengeler.¹⁹ Note the disappearance of the second Pd-Pd shell in PdC_{0.13}, while the higher shells are unaffected. Although this "focusing" effect is usually expected to increase the intensity of the second shell peak,²² it appears that destructive interference between paths containing C atoms and paths not containing C atoms can lead to decreased intensity. We have recently begun to use the latest version (5.03) of FEFF, which includes multiple scattering, to study the effect of multiple scattering by interstitial atoms in Pd hydride, Pd boride, and Pd carbide.

Figure 5 shows representative nonlinear least-squares

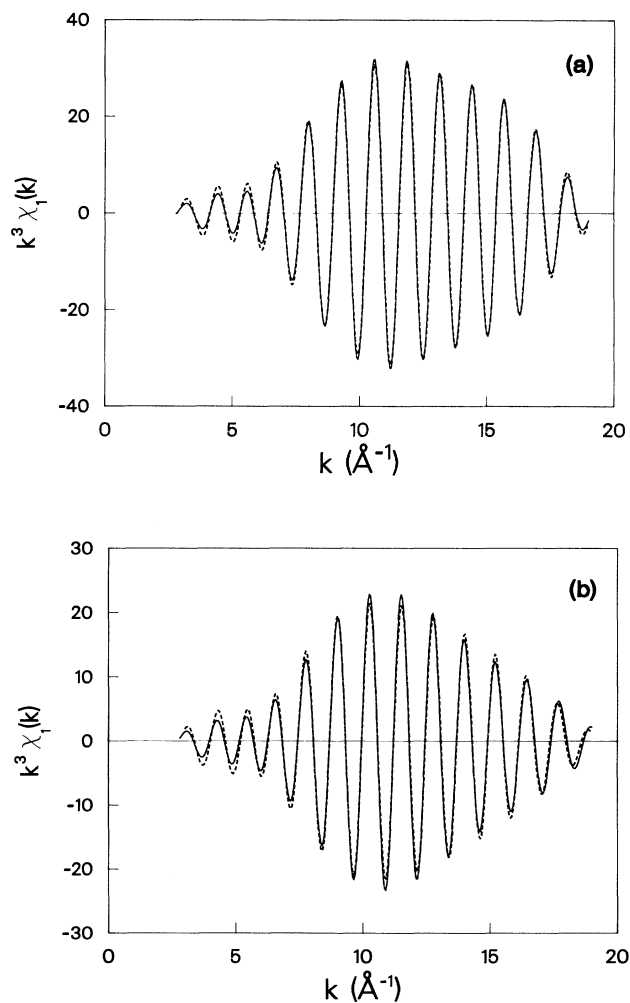


FIG. 5. Least-squares fits to Pd-Pd nearest-neighbor EXAFS, with k^3 weighting, from (a) Pd and (b) PdC_{0.13} powders at 40 K. Solid lines are the Fourier-filtered experimental data; dashed lines are the best fits using a FEFF theoretical standard.

TABLE II. Results of nonlinear least-squares fitting analysis of Pd and PdC_{0.13} EXAFS data using a FEFF theoretical standard. The Pd-Pd coordination number was assumed to be 12 for all the fits.

	T (K)	R (Å)	σ^2 (Å ²)
Pd powder	40	2.743	0.0029
	65	2.742	0.0030
	110	2.742	0.0037
	200	2.741	0.0053
	205	2.741	0.0052
	295	2.738	0.0070
	300	2.732	0.0070
	425	2.732	0.0090
PdC _{0.13} powder	40	2.817	0.0042
	40	2.817	0.0042
	65	2.817	0.0044
	110	2.817	0.0050
	200	2.817	0.0060
	205	2.811	0.0066
	295	2.811	0.0082
	300	2.811	0.0083
	425	2.802	0.010
Pd foil	300	2.730	0.0060

fits to EXAFS from the first Pd-Pd coordination shell of Pd and PdC_{0.13} powders using a theoretical standard generated with FEFF version 3.25. The resulting Pd-Pd distances and Debye-Waller factors are presented in Table II. The apparent contraction of the Pd-Pd distance with increasing temperature is a well-known artifact resulting from neglect of anharmonicity in the EXAFS analysis.²³ At low temperature, 40 K, where the harmonic approximation is expected to be valid, the Pd-Pd distance obtained, 2.743 Å, for Pd powder agrees very well with the known distance 2.744 Å.²⁴ This agreement and the precision demonstrated by observation of a monotonic variation of the Pd-Pd distance shows that the precision of the measurements warrants reporting four significant figures here. Neglect of anharmonicity limits the accuracy of distances obtained at higher temperature to ± 0.02 Å. Those results could be improved by cumulant expansion analysis, as was done by Yokoyama, Kimoto, and Ohta.¹⁵ Of interest here, however, is the measured expansion of the lattice that accompanies carbide formation, 2.7% at all temperatures studied. This agrees well with our XRD results, as well as previously reported XRD and neutron scattering results.^{3,4}

The Pd-Pd distance (2.817 Å) obtained for PdC_{0.13} at 65 K agrees well with that reported by Jones *et al.*, 2.824 Å.¹⁰ Attempts to fit the first Pd-Pd shell with two slightly different distances, as was done by Jones *et al.* (and Lengeler¹⁹ for PdB_x), did not greatly improve the fits, and the resulting distances did not agree well with those reported by Jones *et al.*¹⁰

The Debye-Waller factor of Pd foil at 300 K (0.0060 Å²) agrees well with that reported by Yokoyama, Kimoto, and Ohta (0.0063 Å²).¹⁵ Figure 6 presents the mea-

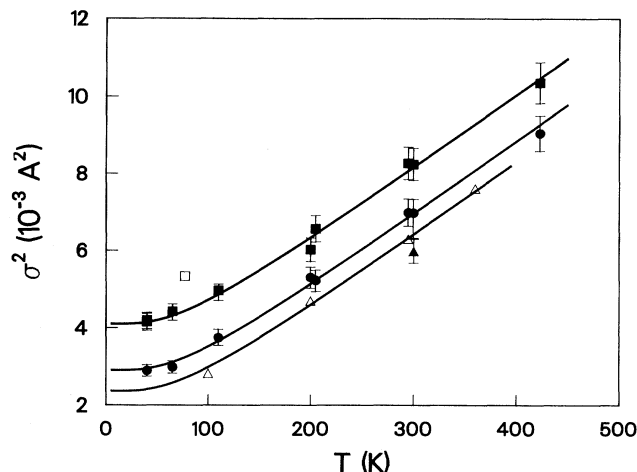


FIG. 6. Mean-squared relative displacement as a function of temperature for Pd (circles) and PdC_{0.13} (squares) powders and Pd foil (triangles). Open triangles are data of Yokoyama, Kimoto, and Ohta (Ref. 15). Open square is a result of Jones *et al.* (Ref. 10). Solid lines are calculated with the correlated Debye model using $\Theta_D = 295$ K plus static disorder contributions of 0.00036, 0.0009, and 0.0023 Å² from bottom to top.

sured Debye-Waller factors for PdC_{0.13} powder, Pd powder, and Pd foil. The error bars reflect an estimated precision of $\pm 5\%$; the absolute uncertainty is expected to be somewhat greater ($\pm 10\%$) since S_0^2 was adjusted to fit the results of Yokoyama, Kimoto, and Ohta. Figure 6 includes the results of Yokoyama, Kimoto, and Ohta for Pd foil and Jones *et al.* for PdC_{0.15}. Note that the temperature dependence (slope above 100 K) is, within experimental error, the same for the powders and foil. The Debye-Waller factor in the standard EXAFS formula is the harmonic approximation of the mean-squared relative displacement. The thermal contribution to the mean-squared relative displacement was calculated using the correlated Debye model as described by Sevillano, Meuth, and Rehr²⁵ and applied recently by Choi *et al.*²⁶ To obtain a good fit to both the Pd and PdC_{0.13} powder data, it was also necessary to include a static (i.e., temperature-independent) contribution to the mean-squared relative displacement. This is normally ascribed to structural disorder. The total mean-squared relative displacement is therefore given by the sum of a thermal and a static contribution.

The best fits are shown in Fig. 6. For both Pd and PdC_{0.13} powder, $\Theta_D = 295 \pm 10$ K; the static contributions to σ^2 are 0.0011 and 0.0023 Å² relative to our result for Pd foil. The estimated uncertainty of Θ_D is based on inspection of the fits obtained with Θ_D varied between 280 and 310 K. The Debye temperature of Pd is greater than that reported by Yokoyama, Kimoto, and Ohta, $\Theta_D = 281$ K, which agreed well with a previously reported thermodynamic value, 275 K.²⁷ However, a better fit (χ^2 reduced by a factor of 2) to the data of Yokoyama, Kimoto, and Ohta is obtained with $\Theta_D = 290$ K if a static contribution to σ^2 of 0.00020 Å² is included. This static contribution could be a systematic error of $\sim 3\%$, well

within the absolute uncertainty of Debye-Waller factor measured by EXAFS, or actual structural disorder in the polycrystalline Pd foil. A recent XRD measurement of Θ_D for nanocrystalline Pd yielded $\Theta_D = 331 \pm 15$ K.²⁸ The Debye-Waller factor obtained for Pd powder at 300 K was consistently greater than that of Pd foil. The EXAFS spectra of Pd powder and foil were obtained simultaneously, so the larger Debye-Waller factor of the Pd powder cannot be attributed to limited spectrometer resolution. Since the Pd powder results parallel those of Yokoyama, Kimoto, and Ohta for Pd foil, the larger Debye-Waller factor at 300 K is ascribed to static, structural disorder in the Pd powder.

Jones *et al.* found $\sigma^2 = 0.0053 \text{ \AA}^2$ for PdC_{0.15} at 77 K, about 20% higher than our result.¹⁰ They did not provide enough detail in that report to comment on the discrepancy. It is almost certainly not due to different carbide stoichiometry since the Pd-Pd distance we obtain agrees well with their result. The temperature dependence of σ^2 of PdC_{0.13} powder is identical to that of Pd powder, yielding $\Theta_D = 295 \pm 10$ K. The additional disorder that accompanies carbide formation is a static contribution, probably the result of local distortion of the lattice around carbon atoms in $\sim 13\%$ of the octahedral interstices. Choi *et al.*, found a similar structural disorder contribution in Pt-Pt EXAFS from Ni₁₀Pt₉₀, where Ni atoms are substitutional “impurities.”

B. XANES results

Figure 7 presents Pd *K*-edge XANES spectra of Pd and PdC_{0.13} powders at 50 K; within 20 eV of E_0 they are nearly identical. The energy scale was calibrated using data acquired simultaneously on a Pd foil at 300 K. E_0 was defined as the first inflection point in the XANES spectrum of Pd metal foil. In all XANES spectra of Pd and PdC_{0.13} powders, the first inflection point was within 0.3 eV of that in the XANES spectrum of Pd metal foil at 300 K. Note that the first inflection point occurs on the rising edge of an unresolved “shoulder” that extends to $\mu x \sim 0.5$ at $E - E_0 \sim 5$ eV. The structure within the edge

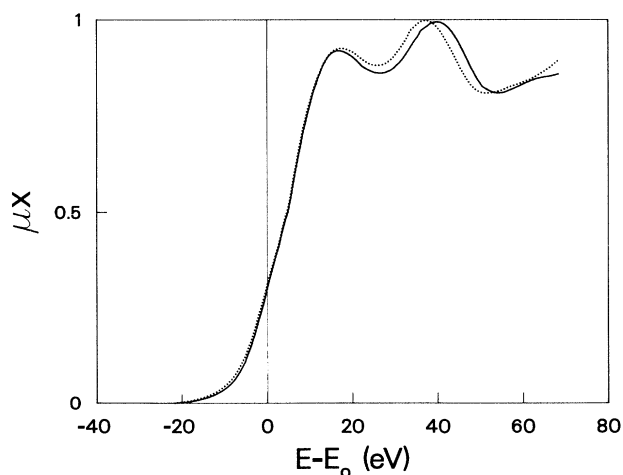


FIG. 7. Pd *K*-edge XANES spectra of Pd (solid line) and PdC_{0.13} (dotted line) powders at 50 K.

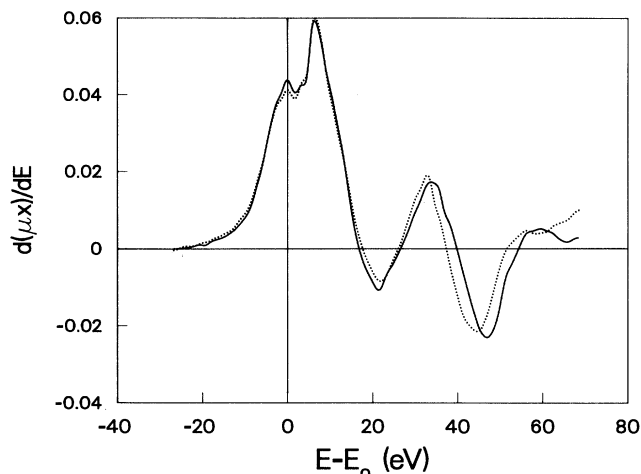


FIG. 8. First derivative plots of Pd *K*-edge XANES spectra (smoothed spline fit) of Pd (solid line) and PdC_{0.13} (dotted line) powders at 50 K.

is more obvious in the first derivative of the XANES spectrum. See Fig. 8. This “shoulder” is the result of $1s \rightarrow 4d, dp$ transitions that are more easily resolved in *K*-edge spectra of lighter 4*d* elements (Y through Ru).²⁹ The same unoccupied final states in Pd are observed as a prominent shoulder in *L*₁-edge spectra ($2s \rightarrow 4d, dp$) of Pd.³⁰ Pd *K*-edge XANES spectra reveal no new unoccupied states in PdC_{0.13}.

Table III presents measured energies of the two lowest-energy absorption maxima in XANES spectra of Pd and PdC_{0.13} powders. The $1s \rightarrow 5p, pd$ peak is at the same energy ($E - E_0 = 16$ eV) in XANES spectra of Pd and PdC_{0.13} powders. The $1s \rightarrow 4f$ peak is shifted slightly upward (~ 0.7 eV) in the spectrum of PdC_{0.13} powder. Davis *et al.* reported that these peaks were not shifted in the Pd *K*-edge XANES spectrum of PdH_{0.66}, but they found that the peaks were narrower than those in Pd metal spectra.³¹ They attributed this to band narrowing caused by lattice expansion (3.7% in PdH_{0.66}). In the

TABLE III. Energies, relative to the first inflection point in the XANES spectrum of Pd foil, of absorption maxima in XANES spectra of Pd and PdC_{0.13} powders.

	<i>T</i> (K)	$1s \rightarrow 5p, pd$ (eV)	$1s \rightarrow 4f$ (eV)
Pd carbide	40	15.9	38.8
	65	15.9	38.6
	110	15.7	38.2
	205	16.0	38.6
	300	16.4	38.9
Average		16.0 ± 0.2	38.6 ± 0.3
PdC _{0.13} powder	40	16.3	39.2
	65	16.3	39.4
	110	15.8	38.9
	205	16.6	39.8
	300	16.2	39.3
Average		16.2 ± 0.3	39.3 ± 0.3

spectra of PdC_{0.13} no narrowing was detected, perhaps because the lattice expansion (2.7% in PdC_{0.13}) is smaller.

The electronic structure of PdC_{0.13} is of interest for understanding suppression of hydride formation by interstitial carbon.⁵ Unfortunately, because of lifetime broadening and limited spectrometer resolution, Pd *K*-edge XANES spectra provide little information. Pd *L*₃-edge XANES (Ref. 32) and valence-band x-ray photoemission³³ have proven more useful for probing the electronic structure of PdH_x. We are currently performing such experiments to characterize the electronic structure of PdC_{0.13}.

V. SUMMARY

The following conclusions are based on this study of the Pd *K*-edge x-ray-absorption spectra of Pd and PdC_{0.13} powders over the temperature range 40–423 K.

(1) The Pd-C coordination shell is not directly visible in a FT of the PdC_{0.13} EXAFS data, because of the low concentration of C and its small backscattering amplitude.

(2) The presence of C atoms in octahedral interstices of the Pd lattice is confirmed by their effect, through multiple scattering, on the intensity of EXAFS from the second Pd-Pd coordination shell.

(3) The measured average lattice expansion, 2.7%, which accompanies carbide formation agrees well with

XRD and neutron scattering results.

(4) The Debye temperature of Pd powder is found to be 295±10 K. Examination of published EXAFS results for bulk Pd foil suggest that it, likewise, has a Debye temperature of ~295 K.

(5) The presence of interstitial C atoms increases the structural disorder, as observed by an increased static Debye-Waller factor, without changing the Debye temperature, $\Theta_D = 295 \pm 10$ K.

(6) The Pd *K*-edge XANES spectrum of PdC_{0.13} powder is nearly identical to that of metallic Pd powder; there is no significant chemical shift of the *K* edge.

(7) Aside from a multiple scattering effect in the second Pd-Pd shell, Pd *K*-edge x-ray-absorption spectroscopy of PdC_{0.13} provides no qualitative signature that could be used for definitive identification.

ACKNOWLEDGMENTS

I acknowledge the help of C. Cook and T. Aversa in performing the experiments and helpful discussions with P. DeGroot, I. Nicolau, and F. Lytle. This research was carried out at beam line X-11A of the National Synchrotron Light Source, which is supported by the U.S. Department of Energy through contracts No. DE-FG05-89ER45384 and No. DE-AC02-76CH00016.

¹S. Nakamura and T. Yasui, *J. Catal.* **17**, 366 (1970).

²S. A. H. Zaidi, *J. Catal.* **68**, 255 (1981).

³S. B. Ziemecki and G. A. Jones, *J. Catal.* **95**, 621 (1985).

⁴S. B. Ziemecki, G. A. Jones, D. G. Swartzfager, R. L. Harlow, and J. Faber, Jr., *J. Am. Chem. Soc.* **107**, 4547 (1985).

⁵J. Stachurski, *J. Chem. Soc., Faraday Trans. I*, **81**, 2813 (1985).

⁶S. B. Ziemecki, G. A. Jones, and D. G. Swartzfager, *J. Less-Common Met.* **131**, 157 (1987).

⁷S. A. H. Zaidi, *Appl. Catal.* **30**, 131 (1987).

⁸S. A. H. Zaidi, *Appl. Catal.* **33**, 273 (1987).

⁹J. A. McCaulley (unpublished).

¹⁰D. J. Jones, J. Roziere, L. E. Aleandri, B. Bogdanovic, and S. Hockett, in *X-ray Absorption Fine Structure*, edited by S. S. Hasnain (Ellis Horwood, New York, 1991), pp. 490–492.

¹¹D. J. Jones, J. Roziere, L. E. Aleandri, B. Bogdanovic, and S. Hockett, *Chem. Mater.* **4**, 620 (1992).

¹²S. M. Heald and D. E. Sayers, *Rev. Sci. Instrum.* **60**, 1932 (1989).

¹³J. J. Rehr, J. Mustre de Leon, S. I. Zabinsky, and R. C. Albers, *J. Am. Chem. Soc.* **113**, 5135 (1991).

¹⁴J. Mustre de Leon, J. J. Rehr, S. I. Zabinsky, and R. C. Albers, *Phys. Rev. B* **44**, 4146 (1991).

¹⁵T. Yokoyama, S. Kimoto, and T. Ohta, *Jpn. J. Appl. Phys.* **28**, L851 (1989).

¹⁶W. H. McMaster, N. Kerr Del Grande, J. H. Mallett, and J. H. Hubbell, *Compilation of X-ray Cross Sections* (National Technical Information Services, Springfield, 1969).

¹⁷D. E. Sayers and B. A. Bunker, in *X-ray Absorption: Principles, Applications, Techniques of EXAFS, SEXAFS, and XANES*, edited by D. C. Koningsberger and R. Prins (Wiley, New York, 1988), pp. 211–253.

¹⁸T. W. Capehart, R. K. Mishra, and F. E. Pinkerton, *Appl.*

Phys. Lett. **58**, 1395 (1991).

¹⁹B. Lengeler, *Phys. Rev. Lett.* **53**, 74 (1984).

²⁰F. Lytle (private communication).

²¹B. Lengeler, *Solid State Commun.* **55**, 679 (1985).

²²E. Stern, in *X-ray Absorption: Principles, Applications, Techniques of EXAFS, SEXAFS, and XANES*, edited by D. C. Koningsberger and R. Prins (Wiley, New York, 1988), pp. 3–51.

²³H. Kuroda, T. Yokoyama, K. Asakura, and Y. Iwasawa, *Faraday Discuss. Chem. Soc.* **92**, 189 (1991).

²⁴Y. S. Touloukian, R. K. Kirby, R. E. Taylor, and P. D. Desai, *Thermophysical Properties of Matter: Thermal Expansion—Metallic Elements and Alloys* (Plenum, New York, 1975), Vol. 12, pp. 248–253.

²⁵E. Sevillano, H. Meuth, and J. J. Rehr, *Phys. Rev. B* **20**, 4908 (1979).

²⁶M. Choi, J. I. Budnick, D. M. Pease, G. H. Hayes, and S. M. Heald, *Phys. Rev. B* **44**, 9319 (1991).

²⁷J. de Launay, in *Solid State Physics: Advances in Research and Applications*, edited by F. Seitz and D. Turnbull (Academic, New York, 1956), Vol. 2.

²⁸J. A. Eastman, M. R. Fitzsimmons, and L. J. Thompson, *Philos. Mag. B* (to be published).

²⁹V. O. Kostroun, R. W. Fairchild, C. A. Kukkonen, and J. W. Wilkens, *Phys. Rev. B* **13**, 3268 (1976).

³⁰T. K. Sham, *Phys. Rev. B* **31**, 1888 (1985).

³¹R. J. Davis, S. M. Landry, J. A. Horsley, and M. Boudart, *Phys. Rev. B* **39**, 10580 (1989).

³²I. Davoli, A. Marcelli, G. Fortunato, A. D'Amico, C. Coluzza, and A. Bianconi, *Solid State Commun.* **71**, 393 (1989).

³³P. A. Bennett and J. C. Fuggle, *Phys. Rev. B* **26**, 6030 (1982).